Zhu et al. Nanoscale Research Letters (2016) 11:198
DOI 10.1186/s11671-016-1419-4

Nanoscale Research Letters

NANO EXPRESS Open Access

Silver Nanoparticles Induce HePG-2 Cells Apoptosis Through ROS-Mediated Signaling Pathways

Bing Zhu[1,2†], Yinghua Li[2†], Zhengfang Lin[2], Mingqi Zhao[2], Tiantian Xu[2], Changbing Wang[2] and Ning Deng[1*]

Abstract

Recently, silver nanoparticles (AgNPs) have been shown to provide a novel approach to overcome tumors, especially those of hepatocarcinoma. However, the anticancer mechanism of silver nanoparticles is unclear. Thus, the purpose of this study was to estimate the effect of AgNPs on proliferation and activation of ROS-mediated signaling pathway on human hepatocellular carcinoma HePG-2 cells. A simple chemical method for preparing AgNPs with superior anticancer activity has been showed in this study. AgNPs were detected by transmission electronic microscopy (TEM) and energy dispersive X-ray (EDX). The size distribution and zeta potential of silver nanoparticles were detected by Zetasizer Nano. The average size of AgNPs (2 nm) observably increased the cellular uptake by endocytosis. AgNPs markedly inhibited the proliferation of HePG-2 cells through induction of apoptosis with caspase-3 activation and PARP cleavage. AgNPs with dose-dependent manner significantly increased the apoptotic cell population (sub-G1). Furthermore, AgNP-induced apoptosis was found dependent on the overproduction of reactive oxygen species (ROS) and affecting of MAPKs and AKT signaling and DNA damage-mediated p53 phosphorylation to advance HePG-2 cells apoptosis. Therefore, our results show that the mechanism of ROS-mediated signaling pathways may provide useful information in AgNP-induced HePG-2 cell apoptosis.

Keywords: Silver nanoparticles, Cellular uptake, Reactive oxygen species, Apoptosis

Background

As one of the most common type of liver cancer, hepatocellular carcinoma (HCC) is the third cause of malignant deaths from cancer-associated worldwide [1–3]. Unfortunately, the diagnosis of HCC is difficult in its earliest stages without screening tests available [4]. Meanwhile, owing to its poor sensitivity to chemotherapeutic agents, high metastatic potential, and resistance to traditional drugs, it is dismal to the overall prognosis of patients with HCC. Thus, it is imperative to develop efficient chemotherapy that has become the great challenge in clinical treatment [5, 6]. In addition, most of current anticancer agents usually have short half-life in the blood circulation and poor aqueous solubility, which hampers therapeutic efficacy of chemotherapy [7, 8]. Recently, nanomaterials have been widely used in biomedical field due to its unique physicochemical properties, including their size distribution, stability of dispersion, morphology, crystalline structure, and thermal properties, that might have the potential to overcome these problems [9]. The increased of application of nanomaterials resulted in raising hopes for employing nanoparticles as alternative anticancer agents [10, 11].

Silver nanoparticles (AgNPs) are less toxic than other form of silver that has obtained an easy access to cells and tissues [12, 13]. AgNPs attract considerable public attention in consumer and medical products compared to other metal materials for their excellent surface enhanced Raman scattering and unique antimicrobial activities [14–17]. Silver nanoparticles have been used widely as antibacterial agents in food storage and environmental [18–21]. Furthermore, AgNPs exhibit low toxicity in humans and have diverse in vitro and in vivo application [22–24]. Moreover, AgNPs have also been shown to combine with corona virus and restrain to

* Correspondence: DengNing123@hotmail.com
†Equal contributors
[1]Guangdong Province Key Laboratory of Molecular Immunology and Antibody Engineering, Jinan University, Guangzhou, Guangdong 510632, People's Republic of China
Full list of author information is available at the end of the article

bind host cells [25]. Thus, exposure to silver nanoparticles as a promising anticancer silver species is becoming increasing intimate and widespread.

Reactive oxygen species (ROS) encompasses highly reactive molecules, including superoxide anion radical, oxygen free radicals, hydroxyl radical, hydrogen peroxide, and singlet oxygen [26]. As a marked imbalance, oxidative stress is the most often described between cellular defense mechanisms and consumption of ROS [27]. The ROS play an important role in many physiological processes. The redox imbalance is associated with many pathologies, such as skin disease, diabetes, cancer, Leigh syndrome, and other diseases [28]. Although many research groups describe the toxicity of AgNP induction of oxidative stress, little is known about the anticancer mechanisms of AgNPs [29]. It is of great interest to ascertain this mechanism of AgNPs. This study was to determine how AgNP-associated changes in redox balance will induce HePG-2 cells apoptosis.

Methods

Materials

HePG-2 cells were purchased from American Type Culture Collection (ATCC, Manassas, Virginia). Fetal bovine serum (FBS) and Dulbecco's modified Eagle's medium (DMEM) were purchased from Gibco. AKT, p53, PARP, and cleaved caspase-3 antibody were obtained from Cell Signaling Technology. Silver nitrate ($AgNO_3$) and vitamin C (VC) were obtained from Sigma. Thiazolyl blue tetrazolium bromide (MTT), 4′6-diamidino-2-phenyindole (DAPI), 2′,7′-dichlorofluorescein diacetate (DCF-DA), bicinchoninic acid (BCA), 6-coumarin, and propidium iodide (PI) were obtained from Sigma. LysoTracker Deep Red was obtained from Invitrogen. The water was supplied by Milli-Q water purification from Millipore in all experiments.

Synthesis of AgNPs

A stock solution of $AgNO_3$ (400 μg/ml) was prepared by dissolving 16 mg $AgNO_3$ powder in 40 ml Milli-Q water. Vitamin C (400 μg/ml) was also prepared by dissolving 16 mg vitamin C in 40 ml Milli-Q water. AgNPs were prepared as follows: briefly, 0.1 ml of 400 μg/ml vitamin C was drop by drop added into 4 ml of 400 μg/ml $AgNO_3$ under magnetic stirring for 2 h. The excess VC and $AgNO_3$ were eliminated by dialysis against Milli-Q water for 24 h. The solution containing nanoparticles was sonicated (KQ-100VDB) by using a water bath for 2 min and pass through filters of 0.2-μm pore size before each experiment. The AgNP concentration was detected by ICP-AES (inductively coupled plasma-atomic emission spectrometry).

Characterization of AgNPs

The morphology of silver nanoparticles was characterized by transmission electron microscope (TEM, Hitachi, H-7650). The size distribution and zeta potential of AgNPs were detected through Zetasizer Nano ZS (Malvern Instruments Limited) particle analyzer. EDX analysis was carried out on an EX-250 system (Horiba) and employed to examine the elemental composition of AgNPs.

Cell Viability Assay

HePG-2 cells were incubated in DMEM supplemented with antibiotic and 10 % FBS, penicillin, and streptomycin in a humidified incubator with 5 % CO_2 atmosphere at 37 °C. The cytotoxicity of AgNPs was detected by MTT assay as previously published [30]. Briefly, cell viability was determined by measuring the ability of cells to transform MTT to a purple formazan dye. HePG-2 cells were seeded in 96-well culture plates at a density of 4×10^4 cells per well at 37 °C for 24 h. Then, the cells were treated with AgNPs at different concentrations for 72 h. After treatment, 20 μl/well of MTT solution (5 mg/ml in PBS) was added and incubated for another 5 h. The medium was removed and replaced with 150 μl/well DMSO to dissolve the formazan crystals. The color intensity of the formazan solution, which reflects the cell viability, was measured at 570 nm using a microplate spectrophotometer (Versammax). The number of test repetitions was three times.

Intracellular Trafficking of AgNPs

To determine the in vitro cellular uptake of AgNPs, the nanoparticles containing a fluorescent dye 6-coumarin were added to the reaction system. The incorporated dye as a probe for AgNPs offers a sensitive method to determine their intracellular localization. The localization of 6-coumarin-labeled 5 μg/ml AgNPs in HePG-2 cells was monitored by DAPI and Lyso Tracker as before [31]. The treated cells cultured in 2-cm cell culture dishes to 70 % confluence were incubated with Lyso Tracker Red (stained for 2 h), and DAPI H33258 was added (stained for 30 min). The cells were rinsed with PBS three times and then incubated with 6-coumarin-loaded AgNPs from 0 to 120 min which were detected by fluorescence microscope.

Flow Cytometric Analysis

Flow cytometric was used to characterize the effect of AgNPs on cell cycle distribution as previously reported [32, 33]. Briefly, the cells incubated with AgNPs for 24 h were collected and centrifuged at 1500 rpm for 5 min. The harvested cells were fixed with pre-cooled 70 % ethanol at −20 °C for 24 h. Cells were followed by PI staining for half an hour in the dark. Apoptotic cells with hypodiploid DNA content were measured by using Multicycle software.

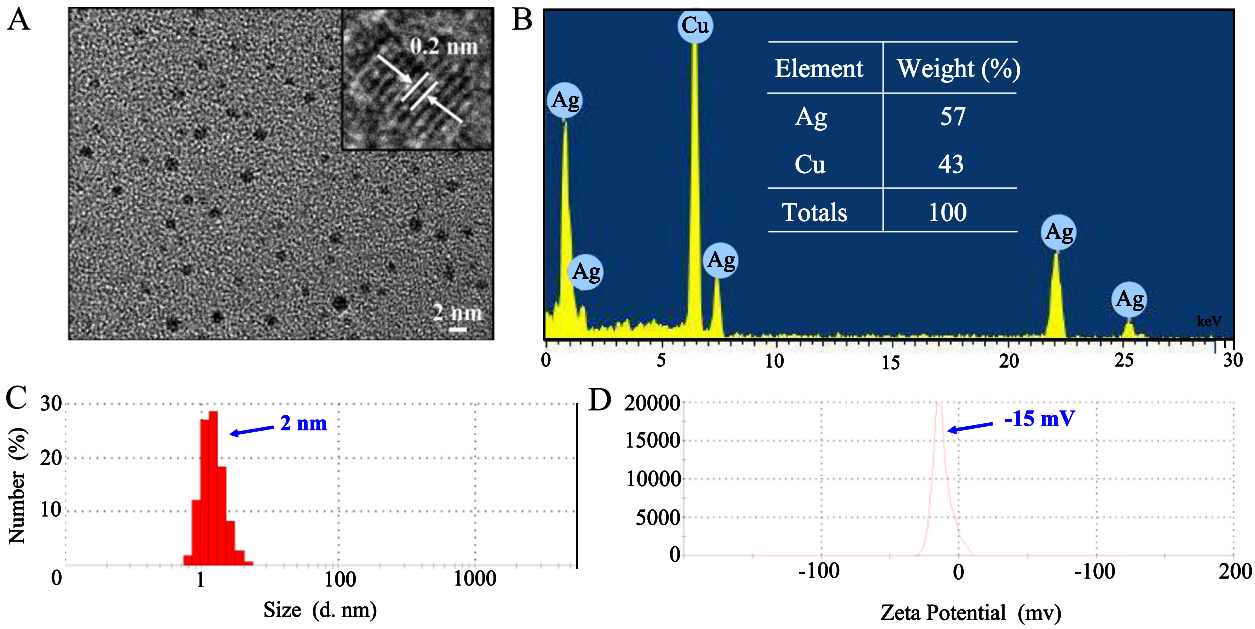

Fig. 1 Structural characterization of AgNPs. **a** TEM image of AgNPs. **b** EDX analysis of AgNPs. **c** Size distribution of AgNPs. **d** Zeta potential of AgNPs

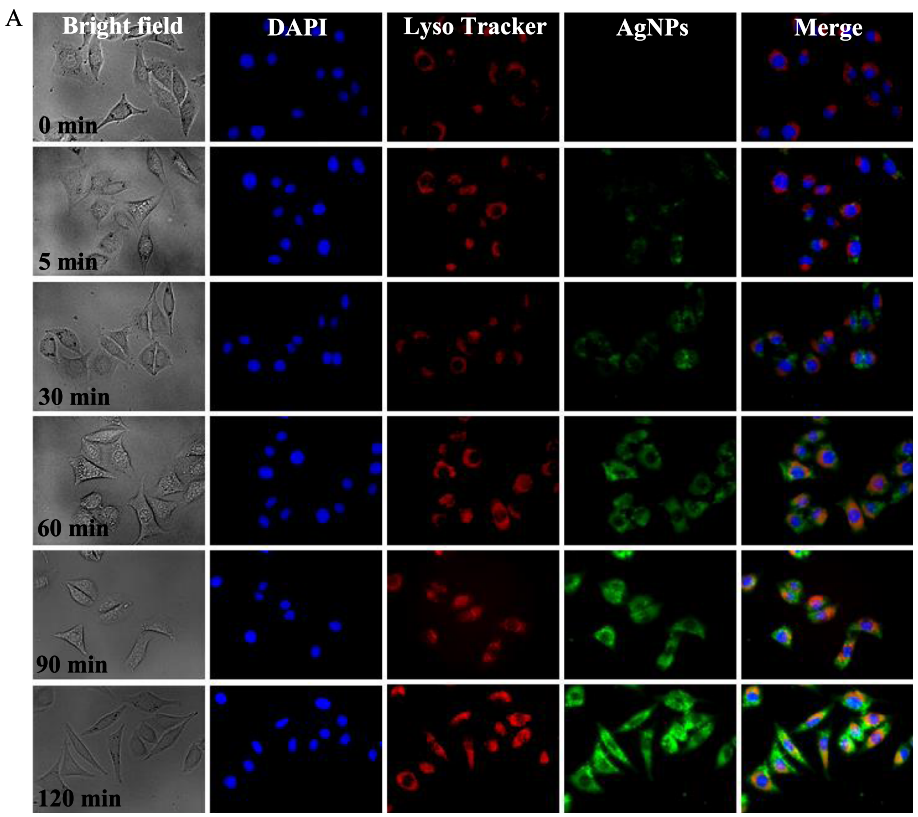

Fig. 2 6-coumarin-labeled AgNPs in HePG-2 cells. The HePG-2 cells were treated with 6-coumarin-marked AgNPs for different periods of time and stained with Lyso Tracker Red (lysosome) and DAPI (nucleus) under fluorescent microscope

Determination of ROS Generation

The intracellular ROS generation by AgNP-treated HePG-2 cells were detected by staining cells with DCF fluorescence as previously reported [34, 35]. Briefly, cells were collected and suspended in PBS with DCFH-DA at a final concentration of 10 mM at 37 °C for 30 min. Then, the stained cells were collected and resuspended in PBS. The ROS level was examined by detecting the fluorescence intensity using fluorescence microscope and microplate reader with excitation an emission wavelengths set at 500 and 529 nm, respectively. Experiments were performed in triplicate.

Western Blotting Analysis

The effects of AgNPs on the expression levels of various intracellular proteins in HePG-2 cells were detected by Western blotting as previously reported [36, 37]. HePG-2 cell treatments with AgNPs were incubated with lysis buffer to obtain total cellular proteins. The protein concentration was examined by BCA assay. Protein (10 μg) was subjected to each well. The membranes were incubated with primary and secondary antibodies at 1:1000 dilution in 5 % non-fat milk. Protein bands were visualized with using enhanced chemiluminescence detection reagent (ECL).

Statistical Analysis

Experiments were performed and repeated at least three times. All the data are presented as mean ± SD. The differences between two groups were analyzed by two-tailed Student's t test. Difference with $P < 0.05$(*) or $P < 0.01$(**) was considered statistically significant. One-way analysis of variance was used in multiple group comparisons. These analyses were carried out using SPSS 13.0 for windows.

Results and Discussion

Preparation and Characterization of AgNPs

In this study, a simple method was used to synthesize AgNPs; various methods were used to characterize the product. As shown in Fig. 1a, TEM images of AgNPs, which demonstrated that the AgNPs presented a uniformity and monodisperse spherical particles, the SAED pattern, and clear lattice fringes (0.2 nm) observed in HRTEM

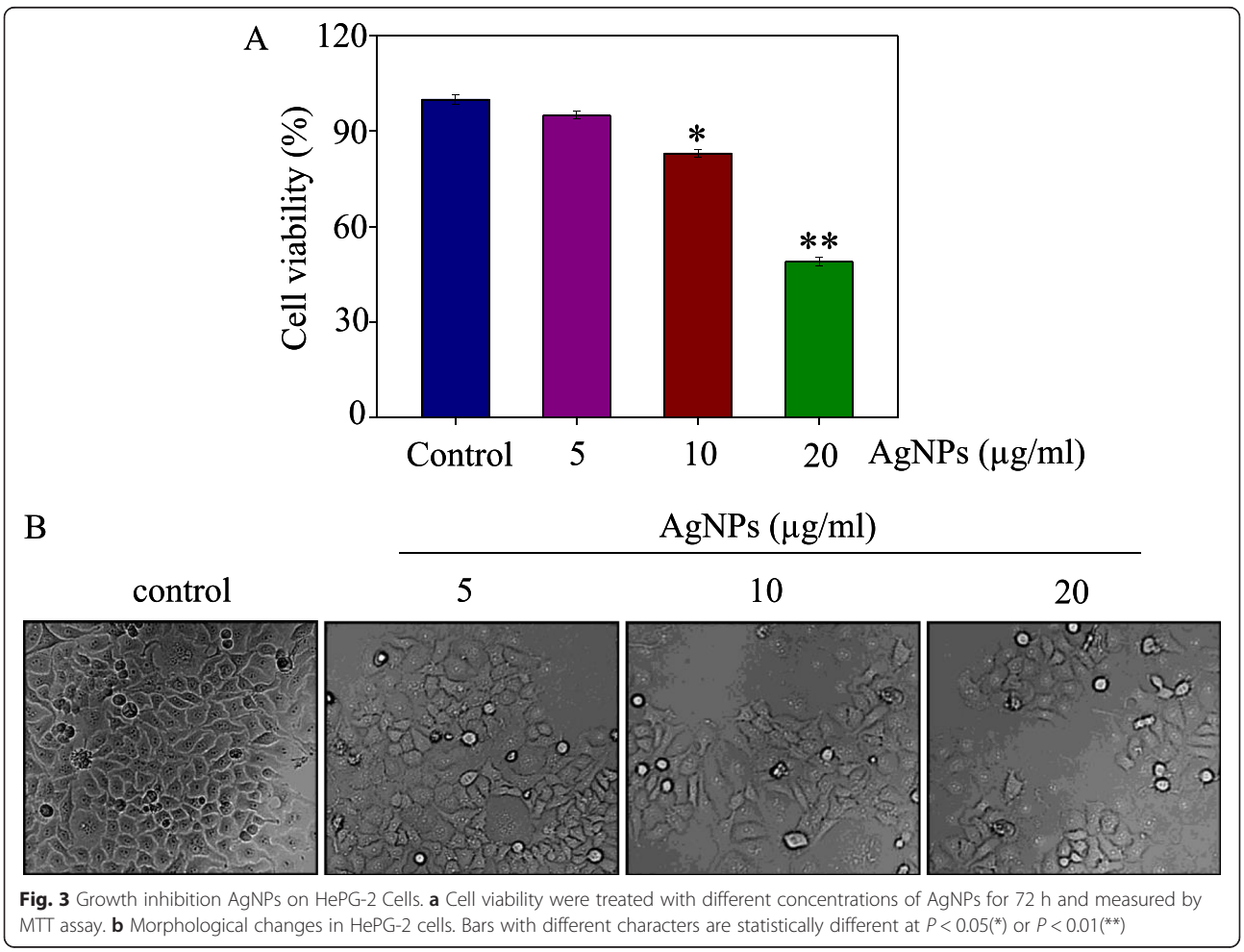

Fig. 3 Growth inhibition AgNPs on HePG-2 Cells. **a** Cell viability were treated with different concentrations of AgNPs for 72 h and measured by MTT assay. **b** Morphological changes in HePG-2 cells. Bars with different characters are statistically different at $P < 0.05$(*) or $P < 0.01$(**)

collectively suggested that the nanoparticle possessed a pure crystal structure. In Fig. 1b, EDX indicated the presence of Ag atoms (57 %) with Cu atom signal (43 %). The presence of Cu comes from copper grids. The atom of Ag indicates that silver nanoparticles were successfully prepared. To examine the effects of stability and surface properties of AgNPs, we detected the size distribution and zeta potential of AgNPs. As shown in Fig. 1c, the average particle size of AgNPs was 2 nm. Furthermore, in Fig. 1d, the zeta potential of AgNPs was −15 mV.

Localization and Uptake Pathways of AgNPs

Endocytosis is one of the primary pathways for cellular uptake of nanoparticles [38]. To examine the intracellular translocation of the nanoparticles, the localization of AgNPs in HePG-2 cells was tracked by simultaneous staining of cell nucleus.

As shown in Fig. 2, the co-localization of AgNPs and lysosomes was found accumulated in HePG-2 cell membrane and gradually enhanced after then. AgNPs escaped from lysosome after 60 min, transported into the cytosol, and distributed in cells after 120 min. This result demonstrates that lysosome is the target organelle of AgNPs.

In Vitro Anticancer Activity of AgNPs

The cytotoxic effect of AgNPs on HePG-2 cells was evaluated by MTT assay. As shown in Fig. 3a, the AgNPs significantly inhibited the growth of HePG-2 cells in a dose-dependent manner.

HePG-2 cells treated with 5 μg/ml AgNPs for 72 h reduced cell viability to 95 %. At the concentrations of 10 and 20 μg/ml, AgNPs decreased the cell viability to 83 and 49 %, respectively. The anticancer activity effects of AgNPs were also further confirmed as shown in Fig. 3b. Cell treated with AgNPs showed cytoplasm shrinkage and loss of cell-to-cell contact. Taken together, these results indicated that AgNPs inhibited cancer cell growth in a dose-dependent manner.

Induction of Cell Apoptosis by AgNPs

Apoptosis plays an essential role in a wide variety of different biological systems, including normal cell cycle, the immune system, embryonic development, morphologic change, and chemical-induced cell death [39]. Therefore, flow cytometry was used to investigate whether apoptosis was involved in cell death by AgNPs. The apoptotic cells which have DNA fragmentation show a typical sub-G1 peak in DNA histogram. As shown in Fig. 4a, b, 5 μg/ml of AgNPs increased the percentage of apoptotic cells to 8.62 %. However, the sub-G1 apoptotic cell population was significantly increased in a dose-dependent manner. At concentrations of 10 and 20 μg/ml, AgNPs increased the apoptotic cells to 19.83

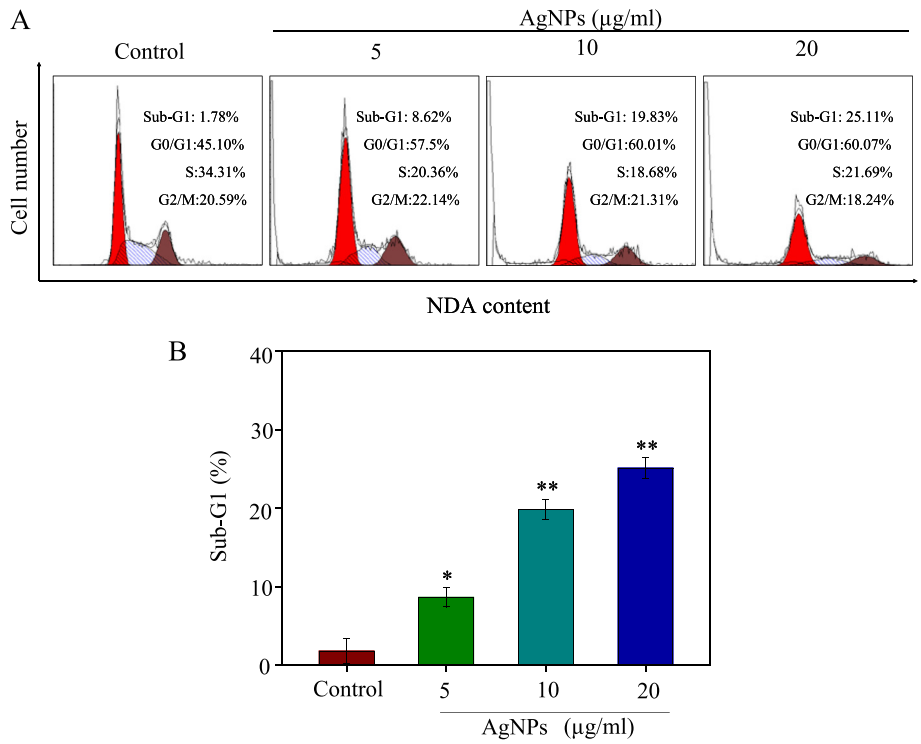

Fig. 4 Flow cytometric analysis of HePG-2 cells after treated with AgNPs for 72 h stained with PI after fixation by 70 % ethanol. As shown in **a** and **b**, the cell cycle distribution after different treatments and apoptotic cell population was determined by PI flow cytometric analysis. Bars with different characters are statistically different at $P < 0.05$(*) or $P < 0.01$(**)

and 25.11 %, respectively. The results indicated that AgNPs depressed HePG-2 cells proliferation.

Induction of ROS Generation by AgNPs

ROS has been regarded as a critical activator of cell apoptosis, especially that induced by anticancer drugs [40]. Therefore, in this study, the ROS generation was determined by DCF fluorescence assay to reveal its role the action mechanisms of AgNPs. As shown in Fig. 5a, b, AgNPs gradually increased the intracellular ROS generation in HePG-2 cells; the stronger fluorescent intensity of DCF was found in HePG-2 cells at the concentration 20 μg/ml. As shown in Fig. 5c, AgNPs increased the intracellular ROS generation to 153, 229, and 290 % at concentration of 5, 10, and 20 μg/ml, respectively. The dates indicate that the involvement of ROS may play an important role in the anticancer action.

Activation of ROS-Mediated Signaling Pathways by AgNPs

Intracellular ROS overproduction could trigger DNA damage and cell apoptosis by activating of AKT, MAPKs, and p53 signaling pathways. The effects on the ROS-mediated downstream pathways were examined by using Western blotting. As shown in Fig. 6a, treatments of cells with AgNPs significantly increased the expression levels of p53. Meanwhile, as a biochemical marker of DNA damage, H_2X was significantly activated by AgNPs. Moreover, as shown in Fig. 6b, AgNP treatment triggered differential effects on JNK, ERK, and p38. AgNPs significantly inhibited total ERK and increased the JNK and p38. Meanwhile, treatment of the cells with AgNPs effectively suppressed the expression levels of total AKT in HePG-2 cells as shown in Fig. 6d. The caspase family exhibits important functions in the regulation process of cell apoptosis. Caspase-3 acts as a central regulator in the signaling network [41]. Therefore, the cleavage of caspase-3 and PARP

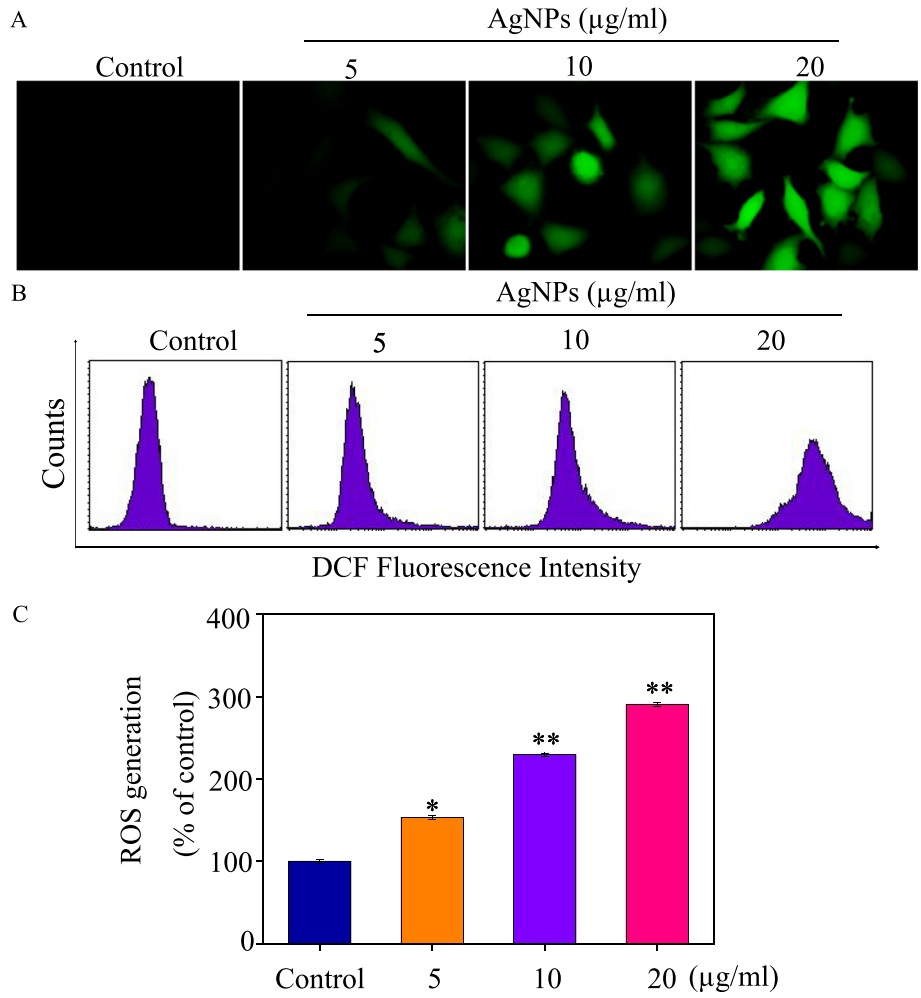

Fig. 5 ROS overproduction induced by AgNPs. **a**–**c** Changes of intracellular ROS generation. ROS levels were detected by DCF fluorescence intensity. Bars with different characters are statistically different at $P < 0.05$(*) or $P < 0.01$(**)

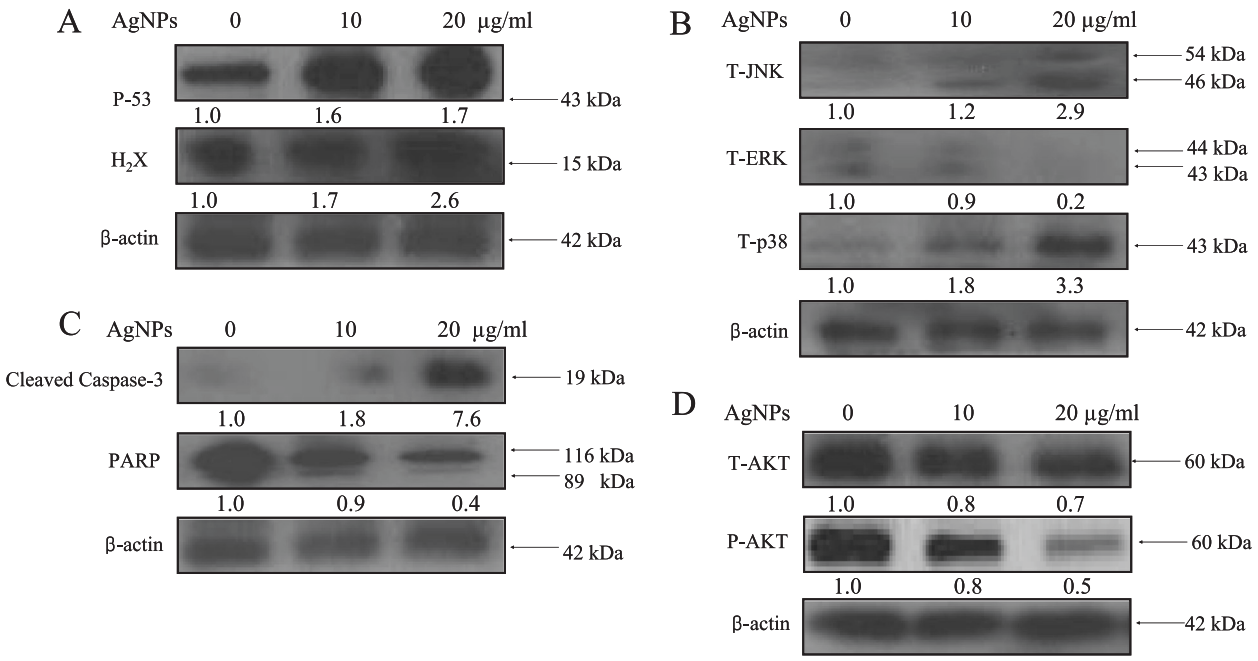

Fig. 6 Activation of apoptotic signaling pathways by AgNPs in HePG-2 cells. **a** DNA damage-mediated p53. **b**–**d** The expression level of MAPKs, caspase-3, and AKT in HePG-2 cells. The *numbers* above the images of bands represent the expression level of protein by densitometry analysis

was examined to evaluate their involvement and contribution to cell apoptosis. As shown in Fig. 6c, AgNPs significantly enhanced the activation of caspase-3 and the cleavage of downstream effect PARP. Taken together, these results support that AgNPs induce HePG-2 cells apoptosis by regulation of ROS-mediated AKT, MAPKs, and p53 signaling pathways.

Conclusions

In summary, a simple chemical method under redox system for preparation of silver nanoparticles has been described in this study. AgNPs exhibit greater abilities to inhibit HePG-2 cells proliferation and enhanced cellular uptake at the average size of 2 nm. AgNPs with dose-dependent manner significantly increased the apoptotic cell population (sub-G1). The studies on the underlying molecular mechanisms revealed that the major mode of cell death induced by AgNPs was cell apoptosis. The mechanisms indicated that AgNPs promote caspase-3-mediated apoptosis by the involvement of ROS generation. Further investigations on apoptotic signaling pathway triggered by the AgNPs in HePG-2 cells are p53, AKT, and MAPKs pathways. Taken together, our findings suggest that AgNP is a prospect silver species with anticancer properties.

Abbreviations

Ag: silver; $AgNO_3$: silver nitrate; AgNPs: silver nanoparticles; DCF-DA: 2',7'-dichlorofluorescein; DMEM: Dulbecco's modified Eagle's medium; FBS: fetal bovine serum; MTT: thiazolyl blue tetrazolium bromide; NPs: nanoparticles; PI: propidium iodide; TEM: transmission electron microscopy; VC: vitamin C.

Competing Interests

The authors declare that they have no competing interests.

Authors' Contributions

BZ and YL designed the study, analyzed the experimental data, and drafted the manuscript. ZL and TX carried out the experiments. MZ and CW participated in its design. ND refined the manuscript and coordination. All authors read and approved the final manuscript.

Acknowledgements

This work was supported by the National Natural Science Foundation of China (NO: 309726300) and the Guangdong Natural Science Foundation (NO: 101 51012001000002).

Author details

[1]Guangdong Province Key Laboratory of Molecular Immunology and Antibody Engineering, Jinan University, Guangzhou, Guangdong 510632, People's Republic of China. [2]Virus Laboratory of Guangzhou Women and Children's Medical Center, Guangzhou, Guangdong 510120, People's Republic of China.

Received: 8 December 2015 Accepted: 5 April 2016
Published online: 14 April 2016

References

1. Chen CL, Tseng YW, Wu JC, Chen GY, Lin KC, Hwang SM et al. (2015) Suppression of hepatocellular carcinoma by baculovirus-mediated expression of long non-coding RNA PTENP1 and microRNA regulation. Biomaterials 44:71–81
2. Shen S, Sun CY, Du XJ, Li HJ, Liu Y, Xia JX et al. (2015) Co-delivery of platinum drug and siNotch1 with micelleplex for enhanced hepatocellular carcinoma therapy. Biomaterials 70:71–83
3. Gopalan B, Narayanan K, Ke ZY, Lu T, Zhang YG, Zhuo L (2014) Therapeutic effect of a multi-targeted imidazolium compound in hepatocellular carcinoma. Biomaterials 35:7479–7487
4. Rand D, Ortiz V, Liu YA, Derdak Z, Wands JR, Taticek M et al. (2011) Nanomaterials for X-ray imaging: gold nanoparticle enhancement of X-ray scatter imaging of hepatocellular carcinoma. Nano Lett 11:2678–2683

5. Ling D, Xia H, Park W, Hackett MJ, Song C, Na K et al. (2014) pH-sensitive nanoformulated triptolide as a targeted therapeutic strategy for hepatocellular carcinoma. ACS Nano 8:8027–8039
6. Thapa RK, Choi JY, Poudel BK, Hiep TT, Pathak S, Gupta B et al. (2015) Multilayer-coated liquid crystalline nanoparticles for effective sorafenib delivery to hepatocellular carcinoma. ACS Appl Mater Inter 7:20360–20368
7. Li LJ, Wang HY, Ong ZY, Xu KJ, Ee PLR, Zheng SS et al. (2010) Polymer- and lipid-based nanoparticle therapeutics for the treatment of liver diseases. Nano Today 5:296–312
8. Wang HL, Thorling CA, Liang XW, Bridle KR, Grice JE, Zhu YA et al. (2015) Diagnostic imaging and therapeutic application of nanoparticles targeting the liver. J Mater Chem B 3:939–958
9. Wu H, Lin J, Liu PD, Huang ZH, Zhao P, Jin HZ et al. (2015) Is the autophagy a friend or foe in the silver nanoparticles associated radiotherapy for glioma? Biomaterials 62:47–57
10. Baek S, Singh RK, Khanal D, Patel KD, Lee EJ, Leong KW et al. (2015) Smart multifunctional drug delivery towards anticancer therapy harmonized in mesoporous nanoparticles. Nanoscale 7:14191–14216
11. Biju V (2014) Chemical modifications and bioconjugate reactions of nanomaterials for sensing, imaging, drug delivery and therapy. Chem Soc Rev 43:744–764
12. Jena P, Mohanty S, Mallick R, Jacob B, Sonawane A (2012) Toxicity and antibacterial assessment of chitosan-coated silver nanoparticles on human pathogens and macrophage cells. Int J Nanomed 7:1805–1818
13. Huo LL, Chen R, Zhao L, Shi XF, Bai R, Long DX et al. (2015) Silver nanoparticles activate endoplasmic reticulum stress signaling pathway in cell and mouse models: the role in toxicity evaluation. Biomaterials 61:307–315
14. Mitrano DM, Rimmele E, Wichser A, Erni R, Height M, Nowack B (2014) Presence of nanoparticles in wash water from conventional silver and nano-silver textiles. ACS Nano 8:7208–7219
15. Chernousova S, Epple M (2013) Silver as antibacterial agent: ion, nanoparticle, and metal. Angew Chem Int Edit 52:1636–1653
16. Han EL, Wu DZ, Qi SL, Tian GF, Niu HQ, Shang GP et al. (2012) Incorporation of silver nanoparticles into the bulk of the electrospun ultrafine polyimide nanofibers via a direct ion exchange self-metallization process. ACS Appl Mater Interfaces 4:2583–2590
17. Tian Y, Qi JJ, Zhang W, Cai Q, Jiang XY (2014) Facile, one-pot synthesis, and antibacterial activity of mesoporous silica nanoparticles decorated with well-dispersed silver nanoparticles. ACS Appl Mater Interfaces 6:12038–12045
18. Cushen M, Kerry J, Morris M, Cruz-Romero M, Cummins E (2014) Evaluation and simulation of silver and copper nanoparticle migration from polyethylene nanocomposites to food and an associated exposure assessment. J Agr Food Chem 62:1403–1411
19. Walser T, Demou E, Lang DJ, Hellweg S (2011) Prospective environmental life cycle assessment of nanosilver T-shirts (vol 45, pg 4570, 2011). Environ Sci Technol 45:7098–7098
20. Anthony KJP, Murugan M, Gurunathan S (2014) Biosynthesis of silver nanoparticles from the culture supernatant of Bacillus marisflavi and their potential antibacterial activity. J Ind Eng Chem 20:1505–1510
21. Gurunathan S, Lee KJ, Kalishwaralal K, Sheikpranbabu S, Vaidyanathan R, Eom SH (2009) Antiangiogenic properties of silver nanoparticles. Biomaterials 30:6341–6350
22. Wang R, Chen CM, Yang WZ, Shi SS, Chen J (2013) Enhancement effect of cytotoxicity response of silver nanoparticles combined with thermotherapy on C6 rat glioma cells. J Nanosci Nanotechnol 13:3851–3854
23. Dipankar C, Murugan S (2012) The green synthesis, characterization and evaluation of the biological activities of silver nanoparticles synthesized from Iresine herbstii leaf aqueous extracts. Colloid Surface B 98:112–119
24. Vasanth K, Ilango K, MohanKumar R, Agrawal A, Dubey GP (2014) Anticancer activity of Moringa olezfera mediated silver nanoparticles on human cervical carcinoma cells by apoptosis induction. Colloid Surface B 117:354–359
25. Lv XN, Wang P, Bai R, Cong YY, Suo SQGW, Ren XF et al. (2014) Inhibitory effect of silver nanomaterials on transmissible virus-induced host cell infections. Biomaterials 35:4195–4203
26. Li YH, Li XL, Zheng WJ, Fan CD, Zhang YB, Chen TF (2013) Functionalized selenium nanoparticles with nephroprotective activity, the important roles of ROS-mediated signaling pathways. J Mater Chem B 1:6365–6372
27. Li YH, Li XL, Wong YS, Chen TF, Zhang HB, Liu CR et al. (2011) The reversal of cisplatin-induced nephrotoxicity by selenium nanoparticles functionalized with 11-mercapto-1-undecanol by inhibition of ROS-mediated apoptosis. Biomaterials 32:9068–9076
28. Zuberek M, Wojciechowska D, Krzyzanowski D, Meczynska-Wielgosz S, Kruszewski M, Grzelak A (2015) Glucose availability determines silver nanoparticles toxicity in HepG2. J Nanobiotechnol 13:72
29. AshaRani PV, Mun GLK, Hande MP, Valiyaveettil S (2009) Cytotoxicity and genotoxicity of silver nanoparticles in human cells. ACS Nano 3:279–290
30. Liu W, Li XL, Wong YS, Zheng WJ, Zhang YB, Cao WQ et al. (2012) Selenium nanoparticles as a carrier of 5-fluorouracil to achieve anticancer synergism. ACS Nano 8:6578–6591
31. Wu HL, Li XL, Liu W, Chen TF, Li YH, Zheng WJ et al. (2012) Surface decoration of selenium nanoparticles by mushroom polysaccharides-protein complexes to achieve enhanced cellular uptake and antiproliferative activity. J Mater Chem 22:9602–9610
32. Yang F, Tang QM, Zhong XY, Bai Y, Chen TF, Zhang YB et al. (2012) Surface decoration by Spirulina polysaccharide enhances the cellular uptake and anticancer efficacy of selenium nanoparticles. Int J Nanomed 7:835–844
33. Xia Y, You P, Xu F, Liu J, Xing F (2015) Novel functionalized selenium nanoparticles for enhanced anti-hepatocarcinoma activity in vitro. Nanoscale Res Lett 10:1051
34. Jiang WT, Fu YT, Yang F, Yang YF, Liu T, Zheng WJ et al. (2014) Gracilaria iemaneiformis polysaccharide as integrin-targeting surface decorator of selenium nanoparticles to achieve enhanced anticancer efficacy. ACS Appl Mater Inter 6:13738–13748
35. He LZ, Huang YY, Zhu HL, Pang GH, Zheng WJ, Wong YS et al. (2014) Cancer-targeted monodisperse mesoporous silica nanoparticles as carrier of ruthenium polypyridyl complexes to enhance theranostic effects. Adv Funct Mater 24:2754–2763
36. Liu T, Zeng LL, Jiang WT, Fu YT, Zheng WJ, Chen TF (2015) Rational design of cancer-targeted selenium nanoparticles to antagonize multidrug resistance in cancer cells. Nanomed-Nanotechnol 11:947–958
37. Huang YY, He LZ, Liu W, Fan CD, Zheng WJ, Wong YS et al. (2013) Selective cellular uptake and induction of apoptosis of cancer-targeted selenium nanoparticles. Biomaterials 34:7106–7116
38. Ma D (2014) Enhancing endosomal escape for nanoparticle mediated siRNA delivery. Nanoscale 6:6415–6425
39. Zhang Y, Li X, Huang Z, Zheng W, Fan C, Chen T (2013) Enhancement of cell permeabilization apoptosis-inducing activity of selenium nanoparticles by ATP surface decoration. Nanomedicine 9:74–84
40. Su J, Lai H, Chen J, Li L, Wong YS, Chen T et al. (2013) Natural borneol, a monoterpenoid compound, potentiates selenocystine-induced apoptosis in human hepatocellular carcinoma cells by enhancement of cellular uptake and activation of ROS-mediated DNA damage. Plos One 8:63502
41. Wang YB, Qin J, Zheng XY, Bai Y, Yang K, Xie LP (2010) Diallyl trisulfide induces Bcl-2 and caspase-3-dependent apoptosis via downregulation of Akt phosphorylation in human T24 bladder cancer cells. Phytomedicine 17:363–368